Astronomy & Astrophysics manuscript no. ISON˙short˙term˙variability˙21jan2015
January 22, 2015

Short-term variability of comet C/2012 S1 (ISON) at 4.8 AU from the Sun

P. Santos-Sanz[1], J.L. Ortiz[1], N. Morales[1], R. Duffard[1], F. Pozuelos[1], F. Moreno[1], and E. Fernández-Valenzuela[1]

Instituto de Astrofísica de Andalucía-CSIC, Glorieta de la Astronomía s/n, 18008-Granada, Spain. e-mail: psantos@iaa.es

Received 3 November 2014 / Accepted 26 December 2014

ABSTRACT

Context. We observed comet C/2012 S1 (ISON) during six nights in February 2013 when it was at 4.8 AU from the sun. At this distance and time the comet was not very active and it was theoretically possible to detect photometric variations likely due to the rotation of the cometary nucleus.
Aims. The goal of this work is to obtain differential photometry of the comet inner coma using different aperture radii in order to derive a possible rotational period.
Methods. Large field of view images were obtained with a 4k × 4k CCD at the f/3 0.77m telescope of La Hita Observatory in Spain. Aperture photometry was performed in order to get relative magnitude variation versus time. Using calibrated star fields we also obtained ISON's R-magnitudes versus time. We applied a Lomb-Scargle periodogram analysis to get possible periodicities for the observed brightness variations, directly related with the rotation of the cometary nucleus.
Results. The comet light curve obtained is very shallow, with a peak-to-peak amplitude of 0.03 ± 0.02 mag. A tentative synodic rotational period (single–peaked) of 14.4 ± 1.2 hours for ISON's nucleus is obtained from our analysis, but there are other possibilities. We studied the possible effect of the seeing variations in the obtained periodicities during the same night, and from night to night. These seeing variations had no effect on the derived periodicity. We discuss and interpret all possible solutions for the rotational period of ISON's nucleus.

Key words. Comets: individual: C/2012 S1 (ISON) – Optical: planetary systems – Methods: observational – Techniques: photometric

1. Introduction

Comet C/2012 S1 (hereafter ISON) was discovered at 6.3 AU from the Sun on September 21, 2012 by V. Nevskiand and A. Novichonok using the International Scientific Optical Network (ISON) near Kislovodsk, Russia (Nevski & Novichonok 2012). The orbit of the comet was quickly computed using precovery images from the Mount Lemmon Survey and Pan-STARRS facilities. The computed orbit was nearly parabolic, which indicated that it was a dynamically new comet coming directly from the Oort cloud, with a nucleus probably including plenty of fresh ices and species (Agúndez et al. 2014) never irradiated by the Sun, like the nucleus of comet C/1995 O1 (Hale-Bopp; A'Hearn et al. 1997). Because of this, a huge outgassing near the perihelion was expected, with a large rate of ice sublimation and dust dragged by the activity from the cometary nucleus. Unfortunately, models that predict the behaviour of a new Oort cloud comet produce large uncertainties when the comet is approaching its perihelion because usually there is no a priori knowledge of many relevant parameters needed for the modelling, and finally ISON's activity close to its perihelion was not so huge as was expected by some initial predictions.

ISON was a sungrazing comet which reached its perihelion on November 28, 2013, when it passed at only 0.012 AU (2.7 R⊙) from the Sun with a V magnitude of ∼ -2 mag according to SOHO/STEREO images (Knight et al. 2013). This very close approach suggested the possibility that the comet could disintegrate near its perihelion, which actually happened: ISON's nucleus did not survive the close approach to the Sun and it totally vanished (Sekanina & Kracht 2014). At the first moment after the perihelion passage, the nucleus –or at least chunks of particles from the nucleus– seemed to have survived, but finally the brightness of ISON faded dramatically in a short period of time (Knight et al. 2013; Combi et al. 2013; Moreno et al. 2014). Numerous amateur and professional astronomers tried to recover the comet some days after the perihelion; however, the results were negative (Sako et al. 2014).

Rotational periods of several cometary nucleii have been obtained by means of time series photometry (Fay & Wisniewski 1978; Jewitt 1990; Meech et al. 1997; Gutiérrez et al. 2003; Snodgrass et al. 2005; Lamy et al. 2005; Snodgrass et al. 2008; Lowry et al. 2012; Mottola et al. 2014). This task is easier when the comet nucleus is not active and there is not a gas/dust coma (i.e. only the bare nucleus), but it is even possible when there is activity and the comet presents a coma. When a comet nucleus is active, the brightness measured in a region close to it will show three types of photometric variability: i) variability due to the rotation of a non-spherical nucleus which reflects different amounts of sunlight depending on the cross section; ii) periodic variations of the gas/dust production due to diurnal insolation; and iii) activity outbursts and/or other random changes. So, ideally, to obtain the variability due to the rotation of the nucleus it is best to observe when there is no coma, but in case of activity it is also

Send offprint requests to: P. Santos-Sanz: psantos@iaa.es

possible to obtain the rotational period of the nucleus by means of the photometry of the inner coma which can inform us about cyclic diurnal activity variations linked to the rotation of the nucleus (Millis & Schleicher 1986; Schleicher et al. 1990).

It is also known that the measured amplitude of the variations may depend on the aperture size used (Meech et al. 1993). Another factor to take into account are the seeing variations during each night and from night to night which might affect the final photometry and might introduce spurious periodicities (Jewitt 1990; Licandro et al. 2000). In our ISON observations at $r_h \sim 4.8$ AU the comet had a coma, but it was in a quiescent state. This allowed us to derive the rotational period by means of aperture photometry. We also analysed the effect in the photometry of the mentioned seeing variations during our observations.

In Sect. 2 we present the information about the acquisition of ISON's images during the observing run. The data reduction and the photometric technique applied are described in Sect. 3. The results obtained for the rotational period of ISON's nucleus, after the application of the Lomb-Scargle periodogram technique, are detailed in Sect. 4 and discussed in Sect. 5. Finally, a summary of the main results of this work is presented in Sect. 6.

2. Observations

ISON was observed for almost six nights in a row on February 8-9 and 11-14, 2013. Images of the comet were obtained from the f/3 0.77m telescope located at La Hita Observatory in Toledo, Spain, for several hours each night, when it was at heliocentric distances (r_h) of 4.84-4.77 AU and at geocentric distance (Δ) of 4.01 AU. The detector used was a 4k × 4k CCD camera which provided a field of view (FOV) of $48.1' \times 48.1'$ with a 0.705 arcsec/pixel scale of image. This scale is enough to provide accurate point spread function (PSF) sampling, even in the best seeing cases. The median seeing during the observations was $4.8''$ (see Table 1).

Integration time was chosen taking into account two factors: i) it had to be sufficiently long to achieve a high enough signal-to-noise ratio (S/N) to study the comet; and ii) it had to be short enough to avoid elongated images of the comet (because the telescope tracked at sidereal speed in order to use the stars in the field to do relative photometry). Considering these two criteria, and the poor median seeing, the integration time chosen was 150 seconds. No binning was used for the image acquisition. During the observing dates the comet was moving at a median speed ~ 0.55 arcsec/min, so it spanned around 2 pixels in the images during the total integration time (i.e. the comet trail is negligible compared with the median seeing, and differential tracking is not needed). Images of the comet were acquired without filter in order to maximize the S/N.

Since the goal of this work is to study the brightness variability of comet ISON, we use relative photometry, not absolute photometry, to search for possible short-term periodicities. Our instrument setup is ideal in this regard because the very large FOV allows us to always use the same reference stars for photometry, at least for several days, which permits a higher photometric precision than absolute photometry. The dates of observations, number of ISON images, geometric data, and night conditions during the observing run are summarized in Table 1.

Table 1. Observational circumstances of comet C/2012 S1 (ISON) during February 2013

Date	JD [days]	images	r_h [AU]	Δ [AU]	α [deg]	FWHM [arcsec]
2013-Feb-08	2456332.47479-2456332.58176	42	4.839	4.010	6.963	4.87
2013-Feb-09	2456333.37477-2456333.62491	97	4.828	4.009	7.169	4.65
2013-Feb-11	2456335.38203-2456335.61912	68	4.806	4.008	7.587	5.30
2013-Feb-12	2456336.40498-2456336.50574	40	4.796	4.008	7.780	5.01
2013-Feb-13	2456337.42286-2456337.60275	76	4.784	4.008	7.996	4.59
2013-Feb-14	2456338.32476-2456338.60417	79	4.773	4.008	8.188	4.14

Date is the date of observation; **JD** is the first and last Julian dates for each observing night; **images** is the number of useful images; r_h **[AU]:** heliocentric distance (AU); Δ **[AU]:** geocentric distance (AU); α**[deg]:** phase angle (degrees); **FWHM:** median of the full width at half maximum of the seeing for each observing night (arcseconds).

3. Data reduction

Series of sky flatfield and bias images were obtained during each observing night to correct the images of the comet. Using these images we built a median bias and a median flatfield for each observing night. We take enough bias and flatfield images so that we can reject those that might be affected by acquisition or observational problems. Each day a median flatfield was constructed using twilight dithered images. The final median flatfield image was inspected for possible residuals from very bright or saturated sources. The flatfield exposure times were long enough to avoid any shutter effect. Each comet image was bias subtracted and flatfielded using the median bias and median flatfield in order to remove image gradients and artefacts. No cosmic ray removal algorithms were used but images with cosmic rays or stars very close to the position of the comet were rejected in order to get the highest quality and uncontaminated photometry.

3.1. Photometry

Daophot routines (Stetson 1987) were used to perform relative photometry using a maximum of 25 stars. The mean error bar of the individual relative magnitudes of the comet was ~ 0.02 mag. Special care was taken not to introduce bad results due to background

sources in the aperture or in the background annulus chosen to compute the sky level. Images affected by cosmic ray hits or artefacts within the flux aperture are not included in our final photometry.

A common reduction software programmed in IDL was used for the photometry of all the previously calibrated images. Trial aperture sizes ranged from 8 to 20 pixels. In general, it was necessary to choose an aperture that was as small as possible to get the highest S/N, but large enough to measure most of the flux. Then we needed to use an aperture radius that was about the same size as the FWHM of the seeing, and to check several aperture radii values around this one. In the case of a comet, even if it is at moderately large heliocentric distances (as was comet ISON when we observed it), activity is expected (i.e. at 4.8 AU no high activity is expected, at least no H2O sublimation, only activity triggered by CO or CO2 sublimation). With all this in mind, we finally found the aperture that gave the lowest dispersion in the photometry of the comet and of the stars with similar brightness. In our particular case we also used a deeper and better space-resolved image of the comet inner coma, acquired with a larger telescope, to help us select the optimum aperture radius. This image was acquired in February 2013, 14.04 UT (Moreno et al. 2014), very close to the dates of our observations. It was taken with the 1.52 m telescope located at Sierra Nevada Observatory and operated by the Instituto de Astrofísica de Andalucía (CSIC) in Spain. We used a 2048×2048 VersArray CCD attached to the telescope in a 2×2 binning mode providing a scale of image of 0.46 arcsec/pixel and a red Johnson-Cousins filter. The seeing during this observing night was 1.63″. The image was processed and filtered with different digital techniques (Samarasinha & Larson 2014) in order to enhance structures in the inner coma; the results of this processing are shown in the four upper panels of Figure 1. A small tail structure or coma enhancement pointing to the antisolar direction is clearly visible in the Larson-Sekanina and Laplacian filtered images. We placed different apertures at the photocentre of the Laplacian filtered image in order to see which aperture radii are affected by the tail or coma structure. As we can see in the figure (blue circles in the bottom panel of Figure 1), the antisunward tail or coma structure is avoided for aperture diameters less than or equal to 5.6″ (i.e. 8 pixels for the plate scale of La Hita Observatory images). We selected this aperture diameter as the best one in order to perform the photometry: it is large enough to include a significant amount of flux ($FWHM_{median}$ = 4.8″) and small enough to avoid the antisunward tail or coma structure.

Several sets of reference stars were used to get the relative photometry, but only the set that gave the lowest scatter was chosen. In some cases, several stars per field had to be rejected from the analysis because they exhibited some variability. The final photometry of ISON was computed taking the median of all the light curves obtained with respect to each reference star. This median technique eliminates spurious results and minimizes the scatter of the photometry.

To perform relative photometry of moving targets we tried, ideally, to keep the same reference stars during the whole campaign. As ISON was not a slow moving target during the observation dates (speed∼ 0.55 arcsec/min), it was not possible to keep the same reference stars during the whole campaign. Nevertheless, because the FOV of the instrument is nearly one degree we were able to use the same reference stars on at least two or three nights, which allows us to obtain high accuracy relative photometry. We link the time series photometry from different sets of nights using images of the same fields acquired under photometric conditions after the observing campaign. We took four images for each night field for the six different date fields during the same photometric night. We used these images to calibrate in flux using the same set of reference stars used to perform the relative photometry of the comet. We also checked the stability of this method using different aperture sizes. Finally, we used the calibration factors obtained from this technique to link the time series photometry of nights with different reference stars in order to avoid small jumps in the photometry.

In Sect. 2 we mentioned that we acquired the comet images with no filter. Using no filter may produce strong fringing effects caused by near-infrared interferences. Luckily, this was not the case for our CCD detector. On the other hand, as we mentioned, obtaining unfiltered images allowed us to reach deeper magnitudes with enough S/N.

4. Results

The time series photometry of the comet obtained as explained in Sect. 3.1 was inspected for periodicities using the Lomb technique (Lomb 1976) programmed as described in Press et al. (1992). The photometry needs some corrections before applying the periodogram analysis: i) first we corrected the Julian dates by subtracting the one-way light-time, which is the elapsed time since light left the comet (i.e. we referenced the time to comet-centre coordinates instead of topocentric ones). Light-time correction during the February 2013 ISON campaign was typically ∼ 33 minutes; ii) we also corrected the relative magnitudes for the changing heliocentric (r_h) and geocentric distances (Δ) by means of the expression

$$m_R(1,1) = -2.5 \cdot log(flux) - n \cdot log(r_h) - 5 \cdot log(\Delta), \quad (1)$$

where $m_R(1,1)$ is the corrected (by r_h and Δ, expressed in astronomical units –AU) relative magnitude, $flux$ is the relative measured flux in ADUs (analogue-to-digital units), and n is an index which reflects the change of the magnitude with the heliocentric distance. This index is usually 5 for asteroids and airless bodies, and can be larger for objects with an atmosphere or an active coma, like active comets. We tried different values for n, from $n = 5$ (i.e. asteroidal behaviour) to $n = 20$ (very active coma or atmosphere). For all these values we obtained compatible results from the Lomb periodogram analysis. Finally we chose $n = 5$ as the preferred value because it implies an asteroidal behaviour, but it is also compatible with a quiescent or stable coma with a nearly constant amount of dust inside the photometric aperture. This choice is supported by the magnitude slope reported by Sekanina & Kracht 2014 for the time of our observations (see Figure 2 of the cited work) when the magnitude changed as r_h^{-5}, which means $n = 5$.

The periodogram obtained after the analysis of these data is shown in Figure 2 and is analysed in Sect. 4.1. Similar periodograms were obtained using different photometric apertures and n-indexes, but we have justified our preferred aperture diameter (5.6″) in Sect. 3.1 and our preferred n-index (n = 5) in the current section.

We have checked as well if the seeing variations from night to night and during the same night may have affected the derived photometry producing spurious periodicities as suggested in the work by Licandro et al. (2000). To discard this effect, we searched for possible correlations between the measured magnitudes and the FWHMs obtained for each image. We do not see any correlation

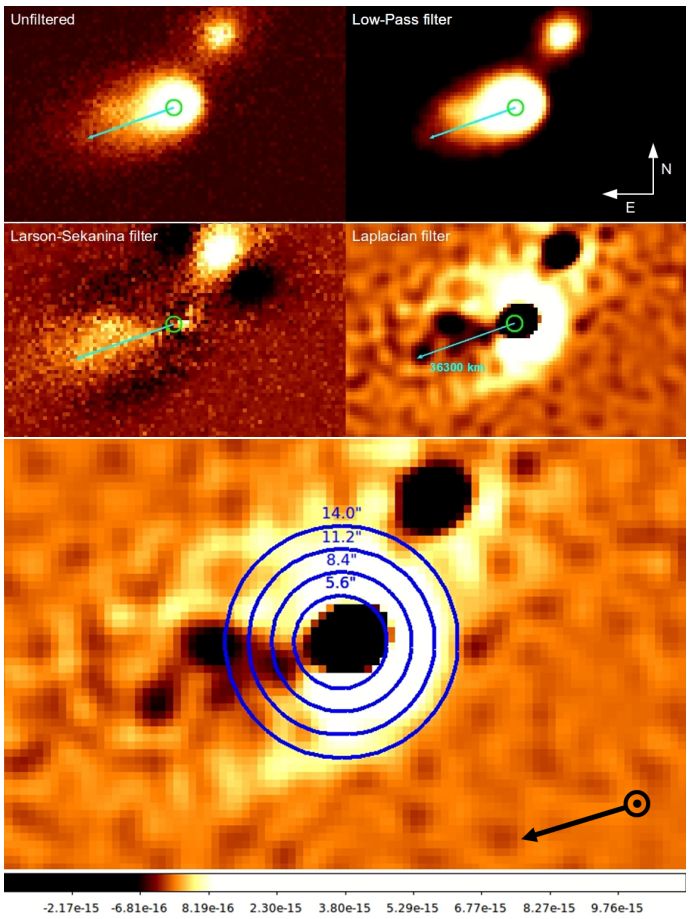

Fig. 1. ISON image from the 1.52 m telescope at Sierra Nevada Observatory taken on February 2013 14.04 UT. **In the upper four panels** the unfiltered image (upper left) and filtered images using different digital techniques: Low Pass, Larson-Sekanina, and Laplacian filters (Samarasinha & Larson 2014). Green circles mark the comet photocentre. Green arrows indicate the small tail or coma enhancement structure pointing to the antisolar direction, clearer in the filtered images, in particular in the Larson-Sekanina and Laplacian ones. **In the bottom panel**, zoom-in of the ISON image processed with the Laplacian filter. Blue circles are the different apertures (diameter in arcseconds) used to perform the photometry. The smallest (aperture = 5.6″) is not contaminated by the small antisunward tail or coma structure. In all panels north is up and east to the left. The antisolar direction is shown with a black arrow.

of the relative magnitudes versus the FWHMs using a Spearman test (Spearman 1904). To be even more confident we search for time periodicities of the FWHMs using the Lomb technique (Lomb 1976) and we do not get any reliable period, so we concluded that the brightness variabilities (and periodicities) observed in our photometric data are real (i.e. due to variability likely related with the rotation of the nucleus) and not due to variations on the weather conditions.

Apart from the relative photometry, we have also estimated absolute photometry using USNO-B1 stars in the FOV as photometric references. With this technique we obtained an estimation of the R magnitudes of comet ISON during our observing campaign, but the uncertainty in the absolute calibration is large, around 0.4 mag because the USNO-B1 magnitudes are not standard BVRI magnitudes and we are not using a filter. In Table 2 (online material) we show the whole time series photometry of comet ISON: dates and R magnitudes for each image. The mean R-magnitude obtained is 16.23 mag. This table also includes $m_R(1,1)$, which are the R magnitudes that ISON would have at 1 AU from the Sun and the Earth (no phase correction applied), and the geometrical circumstances of the comet during the observing dates, such as the phase angle (α), and the heliocentric (r_h) and geocentric (Δ) distances.

4.1. Tentative rotational periods

The main peak in the Lomb-Scargle periodogram (Figure 2) is centred at 1.67 cycles/day (14.4 h) with a normalized spectral power of 50.25. There are what appear to be two 24 h aliases at ±1 cycles/day from the main peak (at 9.0 h and 35.7 h respectively) with smaller spectral power than the primary one. We take 14.4 h as the real rotational period, although these other periods could also be possible, in particular 9.0 h, the one with the second largest spectral power. It is important to note that in time series photometry of low amplitude variability one can sometimes find that the true period corresponds to what appears to be an alias (Ortiz et al. 2007; Thirouin et al. 2010). We estimated the uncertainty in the periods by means of the FWHMs of the main peaks in the Lomb periodogram, and our preferred synodic rotational period is 14.4 ± 1.2 hours. This is a single-peaked rotational period,

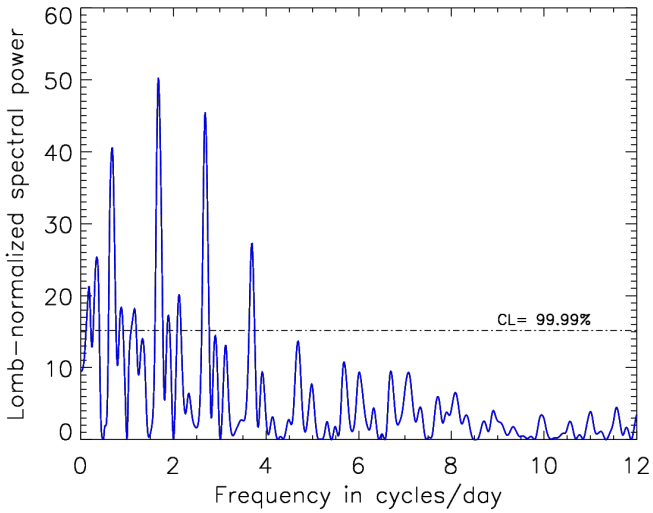

Fig. 2. Lomb-Scargle periodogram from ISON data obtained by means of aperture photometry with an aperture size of 5.6″, and corrected by heliocentric and geocentric distances using Eq. 1. The peak (global maximum) at 1.67 cycles/day with normalized spectral power equal to 50.25 corresponds to a synodic-rotation-period of 14.4 ± 1.2 hours, which we take as our preferred rotational period (see Sect. 4.1 for a detailed explanation). The confidence level above the horizontal dashed line is 99.99%.

which means that the variability could be due to active region(s) distributed along the nucleus producing measurable (though very small) photometric variations in the inner coma. If variability were due to a rotating nucleus with non-spherical shape, the light curve should be double-peaked, and the rotational period should be double, i.e. 28.8 hours. In principle we take the single-peaked solution as the preferred one as is discussed in Sect. 5.

We phased the data described in the first paragraphs of Sect. 4 using the preferred rotational period for ISON's nucleus (14.4 h) and taking 2456332.47479 days as the Julian date for zero phase angle (corresponding to the beginning of our observing run). The resulting rotational light curve is shown in the upper panel of Figure 3. We fitted these data with a one-term Fourier function obtaining the red continuous line shown in the figure. From this Fourier fit we derived a peak-to-peak amplitude (i.e. the full amplitude) of 0.03 ± 0.02 mag. The bottom panel of Figure 3 is the result after applying a running median, with a 0.05 step in phase, to the upper panel light curve. ISON's light curve is cleaner and clearer in this running median curve (Figure 3, bottom panel). The peak-to-peak amplitude derived from a Fourier fit to this median light curve is 0.04 ± 0.02 mag, slightly larger than that derived from the other fit, but compatible within the error bars.

We also built, plotted, and fitted in a similar manner the double-peaked light curve, phasing the data using the 28.8-hour period. The derived peak-to-peak amplitude in this case is exactly the same as for the single-peaked light curve: 0.03 ± 0.02 mag. We did not observe differences among the heights of the two peaks of the double-peaked light curve.

5. Discussion

The observations presented here were obtained from 293 to 287 days prior the perihelion, when comet ISON was not very active and the synthetic aperture CCD photometry technique can be used to extract information of the rotational period of the nucleus. In a recent work about this comet by Sekanina & Kracht 2014 they identify five ignition points which define the comet's brightness/activity evolution from a date before discovery to perihelion. According to this work, our observations were acquired at the end of the second ignition point, when the comet was in a depletion stage, which they call Depletion Stage B, before the next ignition point (see Figure 1 in Sekanina & Kracht 2014). Taking into account these results, the comet nucleus was in a quiescent stage (i.e. no dramatic variation in brightness or in activity) when we acquired ISON's images used in this work. This result supports the conclusion that the variability in the coma photometry we reported is directly related with the rotation of the nucleus and not to activity or outgassing uncoupled from diurnal activity.

On the other hand, Moreno et al. (2014) and Li et al. (2013) claim that comet nucleus illumination geometry was almost constant until the last week before perihelion (i.e. the latitude of the subsolar point remains essentially constant until ∼ 1 AU). This means that almost the same face of the comet was illuminated by the sun until at least $r_h \leq 1$ AU. They also proved, from dust models applied to February 14, 2013, images (Moreno et al. 2014), and by direct detection in Hubble Space Telescope (HST) images from April 10, 2013 (Li et al. 2013), the existence of a jet pointing to the sunward direction with an opening angle ∼ 45°. The fact that the jet morphology did not change during HST and ground-based observations (Knight et al. 2013a) and the small opening angle measured imply that it was a quasi polar jet which constrained the orientation of the nucleus spin axis. We did not detect this quasi-polar sunward jet due to the low resolution of our images. From these results they derived a large obliquity for the spin axis (I ∼ 70° in Moreno et al. 2014, and I = 50°-80° in Li et al. 2013). This large obliquity, jointly with the small phase angle at the dates of our observations (α_{mean} = 7.6°), points to a close to pole-on spin-axis orientation.

The very shallow light curve we calculated, with an amplitude well below 0.1 mag (Δm = 0.03 ± 0.02 mag), could be due to i) a non-spherical nucleus rotating with a small aspect angle, close to a pole-on geometry (i.e. with a spin axis pointing approximately

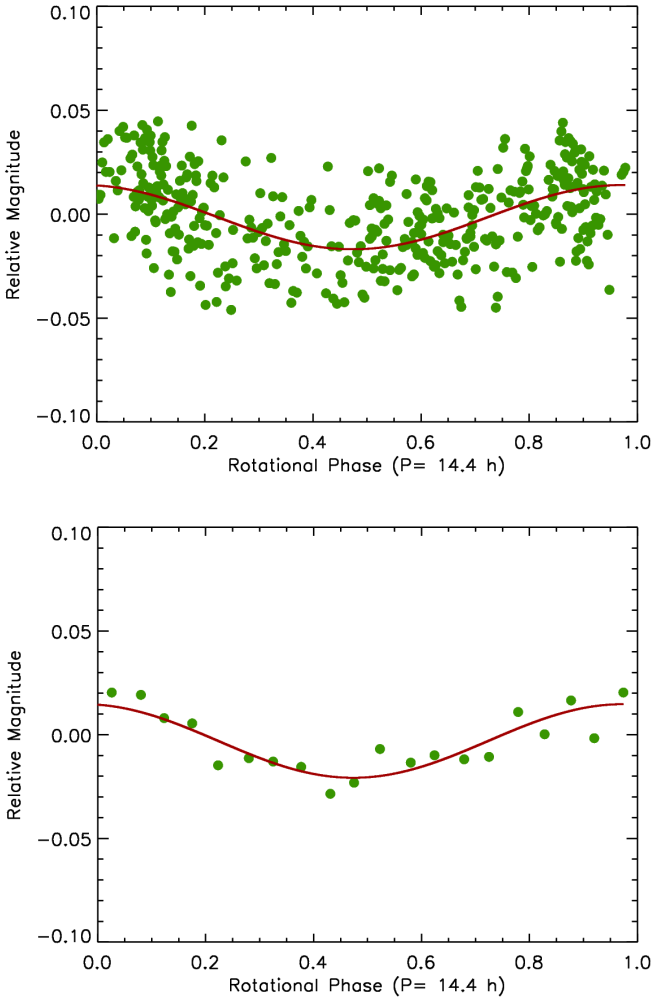

Fig. 3. *Single-peaked light curve of comet ISON.* **Upper panel:** Rotational light curve of comet ISON phasing all the photometric data to the preferred period (14.4 hours). Errors are not plotted for clarity, but each individual value has an uncertainty ~ 0.021 mag. A one-term Fourier fit (red curve) is shown on top of the data, the peak-to-peak amplitude derived from this fit is 0.03 ± 0.02 mag. The Julian date for zero phase angle is 2456332.47479 days. **Lower panel:** Rotational light curve of comet ISON after applying a running median (0.05 step in phase) to the data showed in the upper panel. The rotational light curve variability is clearer to the eye in this plot. Like in the upper panel, a one-term Fourier fit (red curve) is shown on top of the data. Each individual point has an uncertainty ~ 0.015 mag.

towards Earth) whose changing cross section would induce the observed variability, and/or ii) could be produced by a rotating nucleus with different active region(s) distributed along the surface which modulate the inner coma brightness. A combination of i) and ii) could also produce the rotational light-curve that we detected.

We did some calculations in order to quantify the percentage of the amplitude due to a non-spherical rotating nucleus embedded into the coma. Assuming an effective size of 4 km for the nucleus (Li et al. 2013 estimates an upper limit of 4 km for the effective nuclear diameter of ISON) we obtained that a bare nucleus with this effective diameter and a geometric albedo of 5% at r_h = 4.8 AU and Δ = 4.0 AU would have an apparent R-magnitude ~ 21.9 mag. This means that the nucleus would be ~ 190 times fainter than the measured mean R-magnitude of the coma (R ~ 16.2 mag, from the online Table 2); in other words, the contribution of the bare nucleus to the total flux (coma+nucleus) would be ~ 0.5%. With this in mind we estimated the percentage of variation contributed by the bare nucleus (R ~ 21.9 mag) to the total flux (R ~ 16.2 mag), assuming a highly elongated nucleus with an axes ratio of 2 (i.e. assuming a Jacobi ellipsoid shape for the nucleus with axes: $a > b > c$, where c is the spin axis, and $a/b = 2$), and an aspect angle of 90° (which we know was not real because it was close to 0°). Under these assumptions the peak-to-peak amplitude due to the sunlight reflected by such rotating nucleus embedded into the coma is ~ 0.003 mag, which is around 10% of the measured variability of ISON (Δm = 0.03 ± 0.02 mag). As the effective diameter of ISON's nucleus was likely < 4 km (as stated by other authors like Delamere et al. 2013 who estimated D < 1.2 km), the axes ratio (a/b) was probably < 2, and the aspect angle was much smaller than 90°, these estimations are upper limits to the variability produced by the shape of the nucleus. So we conclude that the contribution of the reflected sunlight in the rotating nucleus to the total flux variation would be even smaller than 10%. We can conclude that the variability we measured in the inner coma is probably mainly due to active region(s) in the nucleus with a tiny

and undetectable contribution due to the reflected sunlight in the rotating bare nucleus. These active region(s) located in the rotating nucleus would produce the measured variability, direcly related with the rotational period.

Taking into account the results from the literature we can draw the following scenario during our February 2013 photometric campaign: a cometary nucleus with one of its hemispheres constantly illuminated by the sun, with a highly oblique spin axis pointing to the sun (aspect angle close to 0°) and with a near-pole jet (not visible in our images) observed with a small phase angle from Earth. Under this scenario any change in the activity of the comet happened in the same part of the surface, and was not due to diurnal variations (Li et al. 2013). These authors also state that it is unlikely, under this particular geometry, to have diurnal modulation of activity observable as periodic brightness variations. Nevertheless, we obtained periodic brightness variations with a very low peak-to-peak amplitude which can be consistent with this scenario if the pole is not exactly located at the subsolar point. This would produce periodic exposure to sunlight of small parts of the nucleus compatible with the very low amplitude we get from our data. So it is possible to obtain very low photometric variability related to the rotation of the nucleus under this view.

Finally, a double-peaked light curve is expected for a non-spherical active nucleus if the sublimation comes from the whole surface (i.e. if the object is homogeneously covered of fresh ice). In particular, if variability was mainly due to shape we might expect different heights for the two peaks of the double light curve because a small irregular object does not usually show the same cross section at its maxima. A double-peaked light curve with maxima or minima of different magnitude is not observed. This result also supports the active region-driven variability (single-peaked light curve) against the shape-driven variability (double-peaked light curve). Last, but not least, from photometric analysis of the inner coma of comet C/1995 O1 Hale–Bopp, Ortiz & Rodríguez (1997) obtained a clear synodic single-peaked rotational period of the nucleus of that comet. By similarity with this result –we used the same photometric technique and periodogram analysis for the same type of object, a new comet from the Oort cloud– we also consider that our obtained period for ISON can be interpreted in the same way: it is the synodic single-peaked rotational period of the ISON nucleus, P = 14.4 ± 1.2 h.

6. Summary

Time series photometry of the inner coma of comet C/2012 S1 (ISON) obtained when it was at r_h = 4.8 AU, Δ = 4.0 AU on February 8-9 and 11-14, 2013, are presented and analysed in this work.

We have determined a possible synodic rotational period for the nucleus of comet ISON by means of precise photometry of the inner coma and subsequent analysis searching for periodicities.

Our preferred period from the Lomb-Scargle periodogram analysis is 14.4 ± 1.2 hours (1.67 cycles/day). Although two apparent 24 h aliases of this main periodicity (9.0 h / 35.7 h) are possible solutions as well. The double-peaked period (28.8 h) is also possible, but less likely than the single-peaked solution. The amplitude of the variability is 0.03 ± 0.02 mag.

All these results seem roughly compatible with the derived geometrical configuration and illumination of ISON's nucleus during February 2013 (Li et al. 2013; Moreno et al. 2014).

Acknowledgements. This research was based on data obtained at La Hita observatory which is jointly operated by Astrohita and IAA-CSIC. P. Santos-Sanz would like to acknowledge financial support by the Spanish grants AYA2008-06202-C03-01, AYA2011-30106-C02-01, 2007-FQM2998 and 2012-FQM1776. R. Duffard acknowledges financial support from the MICINN (contract Ramon y Cajal).

References

Agúndez, M., Biver, N., Santos-Sanz, P., Bockelée-Morvan, D., & Moreno, R. 2014, A&A, 564, L2
A'Hearn, M. F., Boehnhardt, H., Kidger, M., & West, R. M. 1997, Earth Moon and Planets, 77,
Combi, M.R. et al. 2013, IAU Circular 9266
Delamere, W. A., McEwen, A. S., Li, J.-Y., et al. 2013, Central Bureau Electronic Telegrams, 3720, 1
Fay, T. D., & Wisniewski, W. 1978, Icarus, 34, 1
Gutiérrez, P. J., de León, J., Jorda, L., et al. 2003, A&A, 407, L37
Jewitt, D. 1990, ApJ, 351, 277
Knight, M. et al. 2013, CBET 3731
Knight, M. M., Schleicher, D. G., Begun, J., et al. 2013, AAS/Division for Planetary Sciences Meeting Abstracts, 45, #407.01
Knight, M. M., & Battams, K. 2014, ApJ, 782, L37
Lamy, P., Toth, I., Fernndez, Y., & Weaver, H. 2005, in Comets II, ed. M. Festou, H. Keller, & H. Weaver, (University of Arizona Press), 223
Li, J.-Y., Kelley, M. S. P., Knight, M. M., et al. 2013, ApJ, 779, L3
Licandro, J., Serra-Ricart, M., Oscoz, A., Casas, R., & Osip, D. 2000, AJ, 119, 3133
Lomb, N. R. 1976, Ap&SS, 39, 447
Lowry, S., Duddy, S. R., Rozitis, B., et al. 2012, A&A, 548, A12
Meech, K. J., Belton, M. J. S., Mueller, B. E. A., Dicksion, M. W., & Li, H. R. 1993, AJ, 106, 1222
Meech, K. J., Bauer, J. M., & Hainaut, O. R. 1997, A&A, 326, 1268
Millis, R. L., & Schleicher, D. G. 1986, Nature, 324, 646
Moreno, F., Pozuelos, F., Aceituno, F., et al. 2014, ApJ, 791, 118
Mottola, S., Lowry, S., Snodgrass, C., et al. 2014, A&A, 569, L2
Nevski, V., & Novichonok, A. 2012, IAU Circular 3238
Ortiz, J. L., & Rodríguez, E. 1997, Earth Moon and Planets, 77, 207
Ortiz, J. L., Santos Sanz, P., Gutiérrez, P. J., Duffard, R., & Aceituno, F. J. 2007, A&A, 468, L13
Press, W. H., Teukolsky, S. A., Vetterling, W. T., & Flannery, B. P. 1992, Cambridge: University Press, —c1992, 2nd ed.,
Sako, S. et al. 2013, CBET 3767
Samarasinha, N. H., & Larson, S. M. 2014, Icarus, 239, 168
Schleicher, D. G., Millis, R. L., Thompson, D. T., et al. 1990, AJ, 100, 896
Sekanina, Z., & Kracht, R. 2014, arXiv:1404.5968
Snodgrass, C., Fitzsimmons, A., & Lowry, S. C. 2005, A&A, 444, 287

Snodgrass, C., Lowry, S. C., & Fitzsimmons, A. 2008, MNRAS, 385, 737
Spearman, C., 1904, The proof and measurement of association between two things, Am. J. Psychol., 57, 72
Stetson, P. B. 1987, PASP, 99, 191
Thirouin, A., Ortiz, J. L., Duffard, R., et al. 2010, A&A, 522, AA93

Table 2. Photometry results. **JD** are the Julian dates corrected for light time at the middle of the exposure for each image; **R** are the R magnitudes computed as explained in Sect. 4. The typical error in these R magnitudes estimations is ~ 0.40 mag, but the relative error in the photometry is ~ 0.02 mag; $\mathbf{m}_R(1,1)$ are ISON's R magnitudes corrected for heliocentric and geocentric distances (not for phase angle). These are the magnitudes that ISON would have at 1 AU from the Sun and the Earth, respectively; r_h**:** heliocentric distance (AU); Δ**:** geocentric distance (AU); α**:** phase angle (degrees).

JD	R	$m_R(1,1)$	r_h	Δ	α
	[mag]	[mag]	[AU]	[AU]	[degrees]
2456332.47479	16.254	9.814	4.840	4.010	6.950
2456332.47681	16.251	9.811	4.840	4.010	6.950
2456332.47881	16.253	9.813	4.840	4.010	6.951
2456332.48083	16.269	9.829	4.840	4.010	6.951
2456332.48286	16.279	9.839	4.840	4.010	6.951
2456332.48488	16.264	9.824	4.840	4.010	6.952
2456332.48689	16.280	9.840	4.840	4.010	6.952
2456332.48891	16.264	9.824	4.840	4.010	6.953
2456332.51314	16.234	9.794	4.839	4.010	6.958
2456332.51716	16.236	9.796	4.839	4.010	6.959
2456332.51919	16.255	9.815	4.839	4.010	6.959
2456332.52119	16.251	9.811	4.839	4.010	6.960
2456332.52323	16.279	9.839	4.839	4.010	6.960
2456332.52523	16.286	9.847	4.839	4.010	6.961
2456332.52726	16.278	9.839	4.839	4.010	6.961
2456332.52928	16.231	9.792	4.839	4.010	6.961
2456332.53130	16.251	9.812	4.839	4.010	6.962
2456332.53332	16.278	9.839	4.839	4.010	6.962
2456332.53534	16.250	9.811	4.839	4.010	6.963
2456332.53735	16.267	9.828	4.839	4.010	6.963
2456332.53938	16.240	9.801	4.839	4.010	6.964
2456332.54139	16.256	9.817	4.839	4.010	6.964
2456332.54339	16.251	9.812	4.839	4.010	6.964
2456332.54541	16.266	9.827	4.839	4.010	6.965
2456332.54742	16.278	9.839	4.839	4.010	6.965
2456332.54946	16.269	9.830	4.839	4.010	6.966
2456332.55147	16.266	9.827	4.839	4.010	6.966
2456332.55348	16.255	9.816	4.839	4.010	6.967
2456332.55551	16.234	9.795	4.839	4.010	6.967
2456332.55752	16.242	9.803	4.839	4.010	6.968
2456332.55955	16.244	9.805	4.839	4.010	6.968
2456332.56159	16.236	9.797	4.839	4.010	6.968
2456332.56359	16.221	9.782	4.839	4.010	6.969
2456332.56559	16.233	9.794	4.839	4.010	6.969
2456332.56763	16.251	9.812	4.839	4.010	6.970
2456332.56965	16.253	9.814	4.839	4.010	6.970
2456332.57169	16.248	9.809	4.839	4.010	6.971
2456332.57372	16.261	9.822	4.839	4.010	6.971
2456332.57573	16.250	9.811	4.839	4.010	6.971
2456332.57774	16.271	9.832	4.839	4.010	6.972
2456332.57975	16.286	9.847	4.839	4.010	6.972
2456332.58176	16.228	9.789	4.839	4.010	6.973
2456333.37477	16.227	9.792	4.830	4.009	7.140
2456333.37679	16.232	9.797	4.830	4.009	7.141
2456333.37882	16.213	9.778	4.830	4.009	7.141
2456333.38084	16.217	9.782	4.830	4.009	7.142
2456333.38287	16.231	9.796	4.830	4.009	7.142
2456333.38490	16.245	9.810	4.830	4.009	7.142
2456333.38691	16.242	9.807	4.830	4.009	7.143
2456333.38895	16.220	9.785	4.830	4.009	7.143
2456333.39096	16.234	9.799	4.830	4.009	7.144
2456333.39299	16.243	9.808	4.830	4.009	7.144

Continued on next page

Table 2 – Photometry results. *Continued from previous page*

JD	R	$m_R(1,1)$	r_h	Δ	α
	[mag]	[mag]	[AU]	[AU]	[degrees]
2456333.39501	16.236	9.801	4.830	4.009	7.145
2456333.39703	16.212	9.777	4.830	4.009	7.145
2456333.42160	16.226	9.791	4.829	4.009	7.150
2456333.42359	16.230	9.795	4.829	4.009	7.151
2456333.42560	16.256	9.821	4.829	4.009	7.151
2456333.42763	16.240	9.805	4.829	4.009	7.151
2456333.42963	16.237	9.803	4.829	4.009	7.152
2456333.43166	16.233	9.799	4.829	4.009	7.152
2456333.43366	16.235	9.801	4.829	4.009	7.153
2456333.43568	16.246	9.812	4.829	4.009	7.153
2456333.43770	16.252	9.818	4.829	4.009	7.154
2456333.43970	16.254	9.820	4.829	4.009	7.154
2456333.44171	16.253	9.819	4.829	4.009	7.155
2456333.44374	16.250	9.816	4.829	4.009	7.155
2456333.44574	16.236	9.802	4.829	4.009	7.155
2456333.44775	16.241	9.807	4.829	4.009	7.156
2456333.44976	16.220	9.786	4.829	4.009	7.156
2456333.45176	16.236	9.802	4.829	4.009	7.157
2456333.45376	16.218	9.784	4.829	4.009	7.157
2456333.45580	16.225	9.791	4.829	4.009	7.158
2456333.48197	16.226	9.792	4.829	4.009	7.163
2456333.48399	16.247	9.813	4.829	4.009	7.164
2456333.48601	16.227	9.793	4.829	4.009	7.164
2456333.48801	16.238	9.804	4.829	4.009	7.164
2456333.49001	16.240	9.806	4.829	4.009	7.165
2456333.49203	16.251	9.817	4.828	4.009	7.165
2456333.49405	16.259	9.825	4.828	4.009	7.166
2456333.49606	16.251	9.817	4.828	4.009	7.166
2456333.49807	16.245	9.811	4.828	4.009	7.167
2456333.50010	16.245	9.811	4.828	4.009	7.167
2456333.50212	16.226	9.792	4.828	4.009	7.167
2456333.50412	16.225	9.791	4.828	4.009	7.168
2456333.50615	16.250	9.816	4.828	4.009	7.168
2456333.50816	16.241	9.807	4.828	4.009	7.169
2456333.51019	16.227	9.793	4.828	4.009	7.169
2456333.51420	16.224	9.790	4.828	4.009	7.170
2456333.51623	16.260	9.826	4.828	4.009	7.170
2456333.51825	16.225	9.791	4.828	4.009	7.171
2456333.52025	16.246	9.812	4.828	4.009	7.171
2456333.52226	16.270	9.836	4.828	4.009	7.172
2456333.52428	16.274	9.840	4.828	4.009	7.172
2456333.52630	16.210	9.776	4.828	4.009	7.173
2456333.52832	16.244	9.810	4.828	4.009	7.173
2456333.53032	16.249	9.815	4.828	4.009	7.173
2456333.53234	16.210	9.776	4.828	4.009	7.174
2456333.53434	16.249	9.815	4.828	4.009	7.174
2456333.53633	16.207	9.773	4.828	4.009	7.175
2456333.53834	16.227	9.793	4.828	4.009	7.175
2456333.54037	16.248	9.814	4.828	4.009	7.176
2456333.54439	16.243	9.809	4.828	4.009	7.176
2456333.54639	16.270	9.836	4.828	4.009	7.177
2456333.54841	16.260	9.826	4.828	4.009	7.177
2456333.55042	16.250	9.816	4.828	4.009	7.178
2456333.55244	16.235	9.801	4.828	4.009	7.178
2456333.55446	16.213	9.779	4.828	4.009	7.179
2456333.55647	16.242	9.808	4.828	4.009	7.179
2456333.55847	16.238	9.804	4.828	4.009	7.179
2456333.56047	16.230	9.796	4.828	4.009	7.180
2456333.56248	16.232	9.798	4.828	4.009	7.180
2456333.56653	16.237	9.803	4.828	4.009	7.181

Continued on next page

Table 2 – Photometry results. *Continued from previous page*

JD	R	$m_R(1,1)$	r_h	Δ	α
	[mag]	[mag]	[AU]	[AU]	[degrees]
2456333.56855	16.238	9.804	4.828	4.009	7.182
2456333.57056	16.240	9.806	4.828	4.009	7.182
2456333.57256	16.255	9.821	4.828	4.009	7.182
2456333.57457	16.262	9.828	4.828	4.009	7.183
2456333.57657	16.246	9.812	4.828	4.009	7.183
2456333.57856	16.250	9.816	4.828	4.009	7.184
2456333.58059	16.234	9.800	4.828	4.009	7.184
2456333.58260	16.256	9.822	4.827	4.009	7.185
2456333.58461	16.273	9.839	4.827	4.009	7.185
2456333.58662	16.278	9.844	4.827	4.009	7.185
2456333.58865	16.259	9.825	4.827	4.009	7.186
2456333.59065	16.267	9.833	4.827	4.009	7.186
2456333.59265	16.265	9.831	4.827	4.009	7.187
2456333.59466	16.275	9.841	4.827	4.009	7.187
2456333.59667	16.273	9.839	4.827	4.009	7.188
2456333.59869	16.239	9.805	4.827	4.009	7.188
2456333.60273	16.216	9.782	4.827	4.009	7.189
2456333.60675	16.241	9.807	4.827	4.009	7.190
2456333.60877	16.263	9.829	4.827	4.009	7.190
2456333.61080	16.230	9.796	4.827	4.009	7.191
2456333.61282	16.243	9.809	4.827	4.009	7.191
2456333.61485	16.215	9.782	4.827	4.009	7.191
2456333.61685	16.213	9.780	4.827	4.009	7.192
2456333.61885	16.228	9.795	4.827	4.009	7.192
2456333.62087	16.232	9.799	4.827	4.009	7.193
2456333.62289	16.244	9.811	4.827	4.009	7.193
2456333.62491	16.235	9.802	4.827	4.009	7.193
2456335.38203	16.272	9.848	4.808	4.008	7.560
2456335.38404	16.242	9.818	4.808	4.008	7.561
2456335.38606	16.245	9.821	4.808	4.008	7.561
2456335.38808	16.245	9.821	4.807	4.008	7.561
2456335.39012	16.241	9.817	4.807	4.008	7.562
2456335.39213	16.253	9.829	4.807	4.008	7.562
2456335.39417	16.241	9.817	4.807	4.008	7.563
2456335.39617	16.259	9.835	4.807	4.008	7.563
2456335.39821	16.243	9.819	4.807	4.008	7.563
2456335.40022	16.249	9.825	4.807	4.008	7.564
2456335.40223	16.259	9.835	4.807	4.008	7.564
2456335.40426	16.240	9.816	4.807	4.008	7.565
2456335.40626	16.252	9.828	4.807	4.008	7.565
2456335.44701	16.247	9.823	4.807	4.008	7.574
2456335.44904	16.248	9.824	4.807	4.008	7.574
2456335.45106	16.250	9.826	4.807	4.008	7.575
2456335.48341	16.216	9.792	4.806	4.008	7.581
2456335.48545	16.244	9.820	4.806	4.008	7.582
2456335.48748	16.239	9.815	4.806	4.008	7.582
2456335.48950	16.268	9.844	4.806	4.008	7.583
2456335.49153	16.249	9.825	4.806	4.008	7.583
2456335.49354	16.270	9.846	4.806	4.008	7.584
2456335.49557	16.264	9.841	4.806	4.008	7.584
2456335.49759	16.264	9.841	4.806	4.008	7.584
2456335.50164	16.254	9.831	4.806	4.008	7.585
2456335.50366	16.256	9.833	4.806	4.008	7.586
2456335.50567	16.265	9.842	4.806	4.008	7.586
2456335.51376	16.246	9.823	4.806	4.008	7.588
2456335.51578	16.242	9.819	4.806	4.008	7.588
2456335.51784	16.264	9.841	4.806	4.008	7.589
2456335.51986	16.268	9.845	4.806	4.008	7.589
2456335.52188	16.240	9.817	4.806	4.008	7.589
2456335.52390	16.265	9.842	4.806	4.008	7.590

Continued on next page

Table 2 – Photometry results. *Continued from previous page*

JD	R	$m_R(1,1)$	r_h	Δ	α
	[mag]	[mag]	[AU]	[AU]	[degrees]
2456335.52596	16.255	9.832	4.806	4.008	7.590
2456335.52800	16.236	9.813	4.806	4.008	7.591
2456335.53000	16.238	9.815	4.806	4.008	7.591
2456335.53203	16.272	9.849	4.806	4.008	7.592
2456335.53403	16.248	9.825	4.806	4.008	7.592
2456335.53606	16.258	9.835	4.806	4.008	7.592
2456335.53811	16.241	9.818	4.806	4.008	7.593
2456335.54013	16.225	9.802	4.806	4.008	7.593
2456335.54216	16.227	9.804	4.806	4.008	7.594
2456335.54419	16.198	9.775	4.806	4.008	7.594
2456335.54622	16.190	9.767	4.806	4.008	7.595
2456335.54825	16.209	9.786	4.806	4.008	7.595
2456335.55027	16.209	9.786	4.806	4.008	7.595
2456335.55228	16.237	9.814	4.806	4.008	7.596
2456335.55435	16.230	9.807	4.806	4.008	7.596
2456335.55635	16.243	9.820	4.806	4.008	7.597
2456335.55836	16.250	9.827	4.806	4.008	7.597
2456335.56038	16.235	9.812	4.806	4.008	7.597
2456335.56240	16.232	9.809	4.806	4.008	7.598
2456335.56444	16.246	9.823	4.806	4.008	7.598
2456335.56649	16.215	9.792	4.806	4.008	7.599
2456335.56851	16.233	9.810	4.805	4.008	7.599
2456335.57052	16.236	9.813	4.805	4.008	7.599
2456335.57255	16.251	9.828	4.805	4.008	7.600
2456335.57459	16.243	9.820	4.805	4.008	7.600
2456335.57662	16.253	9.830	4.805	4.008	7.601
2456335.57865	16.193	9.770	4.805	4.008	7.601
2456335.58067	16.228	9.805	4.805	4.008	7.602
2456335.58267	16.230	9.807	4.805	4.008	7.602
2456335.58472	16.183	9.760	4.805	4.008	7.602
2456335.59685	16.185	9.762	4.805	4.008	7.605
2456335.60699	16.192	9.769	4.805	4.008	7.607
2456335.61302	16.181	9.758	4.805	4.008	7.608
2456335.61506	16.219	9.796	4.805	4.008	7.609
2456335.61912	16.195	9.772	4.805	4.008	7.610
2456336.40498	16.233	9.814	4.796	4.008	7.771
2456336.41103	16.193	9.774	4.796	4.008	7.772
2456336.41303	16.194	9.775	4.796	4.008	7.772
2456336.41503	16.207	9.788	4.796	4.008	7.773
2456336.41706	16.203	9.784	4.796	4.008	7.773
2456336.41907	16.217	9.798	4.796	4.008	7.774
2456336.42108	16.213	9.794	4.796	4.008	7.774
2456336.42310	16.204	9.785	4.796	4.008	7.775
2456336.42513	16.202	9.783	4.796	4.008	7.775
2456336.42714	16.230	9.811	4.796	4.008	7.775
2456336.42917	16.210	9.791	4.796	4.008	7.776
2456336.43118	16.200	9.781	4.796	4.008	7.776
2456336.43321	16.221	9.802	4.796	4.008	7.777
2456336.43521	16.198	9.779	4.796	4.008	7.777
2456336.43721	16.199	9.780	4.796	4.008	7.777
2456336.43921	16.224	9.805	4.796	4.008	7.778
2456336.44124	16.195	9.776	4.796	4.008	7.778
2456336.44328	16.203	9.784	4.796	4.008	7.779
2456336.44527	16.213	9.794	4.796	4.008	7.779
2456336.44729	16.199	9.780	4.796	4.008	7.780
2456336.44929	16.226	9.807	4.796	4.008	7.780
2456336.45130	16.213	9.794	4.796	4.008	7.780
2456336.45333	16.209	9.790	4.796	4.008	7.781
2456336.45536	16.200	9.781	4.796	4.008	7.781
2456336.45737	16.224	9.805	4.796	4.008	7.782

Continued on next page

Table 2 – Photometry results. *Continued from previous page*

JD	R	$m_R(1,1)$	r_h	Δ	α
	[mag]	[mag]	[AU]	[AU]	[degrees]
2456336.45940	16.208	9.789	4.796	4.008	7.782
2456336.46140	16.194	9.775	4.796	4.008	7.782
2456336.46341	16.181	9.762	4.796	4.008	7.783
2456336.46543	16.178	9.759	4.796	4.008	7.783
2456336.46745	16.201	9.782	4.796	4.008	7.784
2456336.46946	16.205	9.786	4.795	4.008	7.784
2456336.47147	16.212	9.793	4.795	4.008	7.785
2456336.47350	16.225	9.807	4.795	4.008	7.785
2456336.47550	16.213	9.795	4.795	4.008	7.785
2456336.47750	16.217	9.799	4.795	4.008	7.786
2456336.47953	16.206	9.788	4.795	4.008	7.786
2456336.48153	16.196	9.778	4.795	4.008	7.787
2456336.50172	16.197	9.779	4.795	4.008	7.791
2456336.50374	16.177	9.759	4.795	4.008	7.791
2456336.50574	16.182	9.764	4.795	4.008	7.792
2456337.42286	16.243	9.829	4.785	4.008	7.978
2456337.42487	16.206	9.792	4.785	4.008	7.978
2456337.42690	16.215	9.801	4.785	4.008	7.979
2456337.42890	16.212	9.798	4.785	4.008	7.979
2456337.43093	16.207	9.793	4.785	4.008	7.980
2456337.43295	16.197	9.783	4.785	4.008	7.980
2456337.43495	16.192	9.778	4.785	4.008	7.980
2456337.43697	16.209	9.795	4.785	4.008	7.981
2456337.43897	16.228	9.814	4.785	4.008	7.981
2456337.44100	16.211	9.797	4.785	4.008	7.982
2456337.44301	16.193	9.779	4.785	4.008	7.982
2456337.44505	16.205	9.791	4.785	4.008	7.983
2456337.44706	16.213	9.799	4.785	4.008	7.983
2456337.44910	16.185	9.771	4.785	4.008	7.983
2456337.45111	16.245	9.831	4.785	4.008	7.984
2456337.45314	16.227	9.813	4.785	4.008	7.984
2456337.45515	16.184	9.770	4.785	4.008	7.985
2456337.45718	16.194	9.780	4.785	4.008	7.985
2456337.45918	16.200	9.786	4.784	4.008	7.985
2456337.46120	16.217	9.803	4.784	4.008	7.986
2456337.46323	16.226	9.812	4.784	4.008	7.986
2456337.46525	16.204	9.790	4.784	4.008	7.987
2456337.46726	16.200	9.786	4.784	4.008	7.987
2456337.47130	16.213	9.799	4.784	4.008	7.988
2456337.47332	16.174	9.761	4.784	4.008	7.988
2456337.47535	16.180	9.767	4.784	4.008	7.989
2456337.47938	16.179	9.766	4.784	4.008	7.990
2456337.48138	16.219	9.806	4.784	4.008	7.990
2456337.48340	16.207	9.794	4.784	4.008	7.990
2456337.48542	16.197	9.784	4.784	4.008	7.991
2456337.48745	16.204	9.791	4.784	4.008	7.991
2456337.48948	16.191	9.778	4.784	4.008	7.992
2456337.49149	16.202	9.789	4.784	4.008	7.992
2456337.49351	16.220	9.807	4.784	4.008	7.992
2456337.49552	16.224	9.811	4.784	4.008	7.993
2456337.50159	16.189	9.776	4.784	4.008	7.994
2456337.51169	16.179	9.766	4.784	4.008	7.996
2456337.51370	16.240	9.827	4.784	4.008	7.997
2456337.51572	16.219	9.806	4.784	4.008	7.997
2456337.51774	16.202	9.789	4.784	4.008	7.997
2456337.51975	16.176	9.763	4.784	4.008	7.998
2456337.52381	16.174	9.761	4.784	4.008	7.999
2456337.52583	16.201	9.788	4.784	4.008	7.999
2456337.52784	16.188	9.775	4.784	4.008	7.999
2456337.52987	16.184	9.771	4.784	4.008	8.000

Continued on next page

Table 2 – Photometry results. *Continued from previous page*

JD	R	$m_R(1,1)$	r_h	Δ	α
	[mag]	[mag]	[AU]	[AU]	[degrees]
2456337.53190	16.175	9.762	4.784	4.008	8.000
2456337.53590	16.195	9.782	4.784	4.008	8.001
2456337.53795	16.213	9.800	4.784	4.008	8.001
2456337.54199	16.214	9.801	4.784	4.008	8.002
2456337.54403	16.214	9.801	4.784	4.008	8.003
2456337.54604	16.199	9.786	4.784	4.008	8.003
2456337.54804	16.194	9.781	4.784	4.008	8.004
2456337.55005	16.202	9.789	4.783	4.008	8.004
2456337.55208	16.178	9.765	4.783	4.008	8.004
2456337.55410	16.177	9.764	4.783	4.008	8.005
2456337.55613	16.192	9.779	4.783	4.008	8.005
2456337.55817	16.238	9.825	4.783	4.008	8.006
2456337.56021	16.221	9.808	4.783	4.008	8.006
2456337.56226	16.206	9.793	4.783	4.008	8.006
2456337.56428	16.225	9.812	4.783	4.008	8.007
2456337.56628	16.210	9.797	4.783	4.008	8.007
2456337.56831	16.222	9.809	4.783	4.008	8.008
2456337.57034	16.239	9.826	4.783	4.008	8.008
2456337.57237	16.185	9.772	4.783	4.008	8.009
2456337.57439	16.191	9.778	4.783	4.008	8.009
2456337.57641	16.185	9.772	4.783	4.008	8.009
2456337.57845	16.204	9.791	4.783	4.008	8.010
2456337.58248	16.233	9.820	4.783	4.008	8.011
2456337.58449	16.236	9.823	4.783	4.008	8.011
2456337.59057	16.180	9.767	4.783	4.008	8.012
2456337.59260	16.190	9.777	4.783	4.008	8.013
2456337.59463	16.191	9.778	4.783	4.008	8.013
2456337.59667	16.201	9.788	4.783	4.008	8.013
2456337.59870	16.205	9.792	4.783	4.008	8.014
2456337.60072	16.202	9.789	4.783	4.008	8.014
2456337.60275	16.213	9.800	4.783	4.008	8.015
2456338.32476	16.224	9.815	4.775	4.008	8.159
2456338.32677	16.229	9.820	4.775	4.008	8.159
2456338.32878	16.211	9.802	4.775	4.008	8.160
2456338.33079	16.234	9.825	4.775	4.008	8.160
2456338.33282	16.236	9.827	4.775	4.008	8.161
2456338.33483	16.241	9.832	4.775	4.008	8.161
2456338.33686	16.217	9.808	4.775	4.008	8.162
2456338.36032	16.225	9.816	4.774	4.008	8.166
2456338.36238	16.234	9.825	4.774	4.008	8.167
2456338.36441	16.208	9.799	4.774	4.008	8.167
2456338.36645	16.212	9.803	4.774	4.008	8.168
2456338.36845	16.190	9.781	4.774	4.008	8.168
2456338.37047	16.206	9.797	4.774	4.008	8.168
2456338.37250	16.230	9.821	4.774	4.008	8.169
2456338.37454	16.248	9.839	4.774	4.008	8.169
2456338.37655	16.217	9.808	4.774	4.008	8.170
2456338.37859	16.226	9.817	4.774	4.008	8.170
2456338.38060	16.217	9.808	4.774	4.008	8.170
2456338.38262	16.247	9.838	4.774	4.008	8.171
2456338.38463	16.243	9.834	4.774	4.008	8.171
2456338.38667	16.195	9.786	4.774	4.008	8.172
2456338.38868	16.202	9.793	4.774	4.008	8.172
2456338.39072	16.196	9.787	4.774	4.008	8.172
2456338.39272	16.232	9.823	4.774	4.008	8.173
2456338.39476	16.224	9.815	4.774	4.008	8.173
2456338.39678	16.207	9.798	4.774	4.008	8.174
2456338.39880	16.200	9.791	4.774	4.008	8.174
2456338.40083	16.241	9.832	4.774	4.008	8.174
2456338.40286	16.226	9.817	4.774	4.008	8.175

Continued on next page

Table 2 – Photometry results. *Continued from previous page*

JD	R	$m_R(1,1)$	r_h	Δ	α
	[mag]	[mag]	[AU]	[AU]	[degrees]
2456338.40490	16.234	9.825	4.774	4.008	8.175
2456338.40693	16.227	9.818	4.774	4.008	8.176
2456338.40896	16.224	9.815	4.774	4.008	8.176
2456338.41097	16.208	9.799	4.774	4.008	8.177
2456338.41297	16.211	9.802	4.774	4.008	8.177
2456338.41502	16.227	9.818	4.774	4.008	8.177
2456338.41704	16.234	9.825	4.774	4.008	8.178
2456338.41904	16.223	9.814	4.774	4.008	8.178
2456338.42106	16.203	9.794	4.774	4.008	8.179
2456338.42308	16.177	9.768	4.774	4.008	8.179
2456338.49481	16.221	9.812	4.773	4.008	8.193
2456338.49684	16.217	9.808	4.773	4.008	8.194
2456338.49888	16.236	9.827	4.773	4.008	8.194
2456338.50089	16.225	9.816	4.773	4.008	8.195
2456338.50293	16.221	9.813	4.773	4.008	8.195
2456338.50497	16.243	9.835	4.773	4.008	8.196
2456338.50701	16.215	9.807	4.773	4.008	8.196
2456338.50902	16.193	9.785	4.773	4.008	8.196
2456338.51103	16.214	9.806	4.773	4.008	8.197
2456338.51306	16.243	9.835	4.773	4.008	8.197
2456338.51508	16.216	9.808	4.773	4.008	8.198
2456338.51708	16.186	9.778	4.773	4.008	8.198
2456338.51913	16.208	9.800	4.773	4.008	8.198
2456338.52116	16.225	9.817	4.773	4.008	8.199
2456338.52319	16.220	9.812	4.773	4.008	8.199
2456338.52521	16.231	9.823	4.773	4.008	8.200
2456338.52725	16.219	9.811	4.773	4.008	8.200
2456338.52925	16.249	9.841	4.773	4.008	8.200
2456338.55550	16.195	9.787	4.772	4.008	8.206
2456338.55753	16.182	9.774	4.772	4.008	8.206
2456338.56160	16.206	9.798	4.772	4.008	8.207
2456338.56362	16.231	9.823	4.772	4.008	8.207
2456338.56562	16.199	9.791	4.772	4.008	8.208
2456338.56766	16.210	9.802	4.772	4.008	8.208
2456338.56969	16.198	9.790	4.772	4.008	8.209
2456338.57169	16.215	9.807	4.772	4.008	8.209
2456338.57372	16.207	9.799	4.772	4.008	8.209
2456338.57573	16.207	9.799	4.772	4.008	8.210
2456338.57777	16.197	9.789	4.772	4.008	8.210
2456338.57983	16.227	9.819	4.772	4.008	8.211
2456338.58185	16.231	9.823	4.772	4.008	8.211
2456338.58389	16.225	9.817	4.772	4.008	8.211
2456338.58593	16.203	9.795	4.772	4.008	8.212
2456338.58796	16.184	9.776	4.772	4.008	8.212
2456338.58998	16.212	9.804	4.772	4.008	8.213
2456338.59200	16.248	9.840	4.772	4.008	8.213
2456338.59403	16.230	9.822	4.772	4.008	8.213
2456338.59606	16.187	9.779	4.772	4.008	8.214
2456338.60015	16.181	9.773	4.772	4.008	8.215
2456338.60417	16.188	9.780	4.772	4.008	8.215